Published in final edited form as:

Neuron. 2016 September 7; 91(5): 1137–1153. doi:10.1016/j.neuron.2016.07.038.

Identification of Early RET+ Deep Dorsal Spinal Cord Interneurons in Gating Pain

Lian Cui[1,#], **Xuerong Miao**[2,#], **Lingli Liang**[2], **Ishmail Abdus-Saboor**[1], **William Olson**[1], **Michael S Fleming**[1], **Minghong Ma**[1], **Yuan-Xiang Tao**[2,*], and **Wenqin Luo**[1,*]

[1]Department of Neuroscience, Perelman School of Medicine, the University of Pennsylvania. Philadelphia, PA, 19104

[2]Department of Anesthesiology, New Jersey Medical School, Rutgers, the State University of New Jersey. Newark, NJ, 07103

Abstract

The gate control theory (GCT) of pain proposes that pain- and touch-sensing neurons antagonize each other through spinal cord dorsal horn (DH) gating neurons. However, the exact neural circuits underlying the GCT remain largely elusive. Here, we identified a new population of deep layer DH (dDH) inhibitory interneurons that express the receptor tyrosine kinase *Ret* neonatally. These early RET+ dDH neurons receive excitatory as well as polysynaptic inhibitory inputs from touch- and/or pain-sensing afferents. In addition, they negatively regulate DH pain and touch pathways through both pre- and postsynaptic inhibition. Finally, specific ablation of early RET+ dDH neurons increases basal and chronic pain, whereas their acute activation reduces basal pain perception and relieves inflammatory and neuropathic pain. Taken together, our findings uncover a novel spinal circuit that mediates crosstalk between touch and pain pathways and suggest that some early RET + dDH neurons could function as pain “gating” neurons.

Introduction

Noxious stimuli to our body are first detected by primary pain-sensing neurons (nociceptors) in the dorsal root ganglion (DRG), whose central projections terminate in superficial layers (I and II) of the spinal cord dorsal horn (DH). The nociceptive information is then transmitted to DH projection neurons and relayed to the brain (Basbaum et al., 2009). Although designated somatosensory neurons and spinal cord circuits exist for mediating pain sensation, they are modulated by other somatosensory pathways for normal perception (Ma, 2012). Specifically, Aβ low-threshold mechanoreceptors (Abraira and Ginty, 2013;

*Correspondence to: Dr. Yuan-Xiang Tao (yt211@njms.rutgers.edu) and Dr. Wenqin Luo (luow@mail.med.upenn.edu).
#These two authors contribute equally to this work.

Author Contributions

L.C., X.M., M.M., Y.X.T., and W.L. designed experiments; L.C., X.M., L.L., I.A.S., W.O., and M.S.F. conducted experiments; L.C., I.A.S., X.M., L.L., Y.X.T., and W.L. prepared the draft manuscript; all authors read and edited the manuscript.

Fleming and Luo, 2013), which innervate deep DH (dDH) layers (III through V) of the spinal cord and mediate light touch sensation, have been considered important players in nociceptive modulation and mechanical allodynia (Campbell et al., 1988; Truini et al., 2013). A prominent idea is the "gate control theory" of pain (GCT) (Figure 1A), which proposes that some DH inhibitory interneurons (gating neurons) receive excitatory inputs from large-diameter (A) touch-sensing afferents and inhibitory inputs from small-diameter (C) pain-sensing afferents, and that the activation of these gating neurons inhibits transmission of both pain and touch pathways to the DH nociceptive projection neurons (Melzack and Wall, 1965). However, the exact neuronal circuits underlying the GCT have remained largely elusive.

Recent work from different laboratories provides evidence in support of the GCT. For example, Aβ touch fibers were found to have polysynaptic excitatory connections onto superficial DH projection neurons, which are normally under strong inhibition (Bardoni et al., 2013; Torsney and MacDermott, 2006). In addition, a series of recent studies characterized the circuitry and function of several molecularly defined populations of DH interneurons in mediating and modulating touch and pain sensation, including PKCγ+, RORα+, VGLUT3+, and somatostatin (SST)+ excitatory interneurons, and dynorphin (Dyn)+, parvalbumin (PV)+, TRPV1+, and GLYT2+ inhibitory interneurons(Bourane, 2015; Duan et al., 2014; Foster et al., 2015; Kim et al., 2012; Lu et al., 2013; Peirs et al., 2015; Petitjean et al., 2015). Nevertheless, the neural circuits underlying one key prediction of the GCT, activation of nociceptive C fibers will dis-inhibit "gating" neurons (open the "gate"), remain unclear.

Here we identified a new population of molecularly defined dDH inhibitory interneurons, which express the receptor tyrosine kinase *Ret* neonatally (early RET+ dDH neurons). The early RET+ dDH neurons receive excitatory as well as polysynaptic inhibitory inputs from A and C primary afferents. Interestingly, most early RET+ dDH neurons receive inhibitory inputs from other early RET+ dDH neurons, which may allow them to function as an antagonization switch between the C and A pathways. In addition, early RET+ dDH neurons inhibit PKCγ+ and SST+ excitatory interneurons and Aβ and C primary afferents presynaptically. Moreover, activation of early RET+ dDH neurons reverses the DH hyperactivity upon dis-inhibition. Lastly, mice with specific ablation of early RET+ dDH neurons display increased basal pain perception and exacerbated inflammatory and neuropathic pain, whereas acute activation of these neurons reduces basal pain perception and relieves inflammatory and neuropathic pain. Together, our results reveal a novel spinal cord circuit that mediates the crosstalk between pain and touch pathways.

Results

Neonatal Expression of *Ret* Defines a Population of Deep Layer DH Neurons

To search for potential gating neurons that can mediate the crosstalk between pain and Aβ touch pathways, we focused on DH neurons located in layers III through V, where Aβ low-threshold mechanosensory afferents innervate. We noticed that the receptor tyrosine kinase *Ret* is highly expressed in this spinal cord region in neonatal mice (Figure 1B). To reveal the full expression pattern of *Ret* in the dorsal spinal cord, we conducted *in situ* hybridization at

different spinal cord levels and postnatal ages (Figures S1A–O). *Ret* is enriched in deep DH layers when mice are 1 postnatal week (pw) and younger. Around 2pw, expression of *Ret* expands into superficial layers; and at 3pw, DH expression of *Ret* is greatly reduced and stays at a low level.

Ret expansion into the superficial DH layers at 2pw could be due to either dynamic expression of *Ret* in DH cells or migration of early RET+ dDH cells into the superficial layers. To distinguish between these two possibilities, we permanently label early RET+ dDH cells with Tdt by treating $Ret^{Ert2/+};Rosa^{Tdt(f)/+}$ mice with tamoxifen at embryonic day 18 (E18) (Luo et al., 2009). We followed Tdt+ DH cells up to 5pw and found that most of them are still located in deep layers (Figures S1P–Z). This result suggests that *Ret* expansion at 2pw and later is due to a later wave of *Ret* expression in superficial DH cells. Thus, neonatal expression of *Ret* defines a population of deep DH neurons (early RET+ dDH neurons), and *Ret* can be used as a molecular handle to specifically label and manipulate these neurons.

Early RET+ dDH Neurons Make up a Distinct Population of Inhibitory Interneurons

To gain further insight into early RET+ dDH neurons, we conducted double fluorescent *in situ* hybridization of *Ret* with several spinal neuron markers at postnatal day 1 (P1). We found that most RET+ neurons co-express the inhibitory neuron marker *Vgat* (Figure 1C), but not the excitatory neuron marker *Vglut2* (Figure 1F), which suggests that they are inhibitory interneurons. In addition, RET+ neurons co-express *Gad1*, *Gad2* (Figure 1D) and *Glyt2* (Figure 1E), indicating that they could release GABA and/or glycine as neurotransmitters. Moreover, we crossed a Ret^{CFP} knock-in allele (Uesaka et al., 2008) into $Vgat^{Cre};Rosa^{Tdt(f)/+}$ mice, in which all inhibitory neurons are genetically labeled with Tdt while all RET+ cells are labeled by a cyan fluorescent protein (CFP), and co-stained spinal cord sections with the pan-neuronal marker NeuN (Figures 1G–I). Approximately 93.9 ± 0.7% of CFP+ cells are NeuN+, and around 92.9% ± 1.0% of CFP+ cells are Tdt+, indicating that most early RET+ dDH cells are indeed inhibitory neurons (Figure 1J). Conversely, the early RET+ dDH neurons make up about one third of the total deep layer inhibitory interneurons (Figure 1K). To determine whether early RET+ dDH neurons change their properties during postnatal development, we genetically traced early *Ret*+ dDH neurons using the $Ret^{Ert2/+};Rosa^{Tdt(f)/+}$ mice and conducted double fluorescent *in situ* at 3pw. We found that the majority of Tdt+ neurons still express inhibitory neuron markers by 3pw, and that 61.3±2.7% of them are RET+ (Figures S2A–J). Our results indicate that early RET+ dDH neurons continue to be dDH inhibitory neurons at juvenile and adult stages.

In addition, we found that early RET+ dDH neurons do not express opioid-like peptides, such as *dynorphin (Dyn)* and *Enkephalin* (Figures S1AA–DD). Since most early RET+ dDH neurons retain expression of *Ret* at 3pw (Figure S2A–B), we predict that these neurons can be genetically traced using either $Ret^{Ert2/+};Rosa^{Tdt(f)/+}$ or $Ret^{CFP/+}$ mice in the adult. Indeed, we found very similar molecular profiles in adult RET+ dDH neurons of $Ret^{Ert2/+};Rosa^{Tdt(f)/+}$ and $Ret^{CFP/+}$ mice: 25% to 30% overlap between RET+ dDH neurons and PV (Figure S2W) but no overlap with nNOS or PKCγ (Figures S2K–V). Together, our

molecular characterizations suggest that early RET+ dDH neurons make up a unique population of dDH inhibitory neurons.

Intrinsic Firing Properties and Morphologies of Early RET+ dDH Neurons

To reveal the intrinsic firing properties of RET+ dDH neurons, we performed whole cell patch clamp recordings with Tdt+ or CFP+ dDH neurons using spinal cord slices of 4pw $Ret^{Ert2/+}; Rosa^{Tdt(f)/+}$ or $Ret^{CFP/+}$ mice (Figures S3A–F). RET+ dDH neurons display four types of firing patterns upon current injection: tonic firing, delayed firing, phasic firing, and single spike firing (Figure 2A–D). Consistent with their molecular profiles as inhibitory neurons, 64.5% of RET+ dDH neurons in $Ret^{Ert2/+}; Rosa^{Tdt(f)/+}$ mice (Figure 2E) and 80% of those in $Ret^{CFP/+}$ mice (Figure 2F) showed a tonic firing, which is characteristic of inhibitory interneurons (Yasaka et al., 2010). The similar intrinsic properties of RET+ dDH neurons in both mouse lines (Figures 2E–F) further support that a largely overlapping population of dDH neurons are genetically traced by $Ret^{Ert2/+}$ and $Ret^{CFP/+}$ mice.

To characterize the morphologies of early RET+ dDH neurons, we sparsely labeled these neurons by injecting diluted AAV1-Flex-ChR2-EYFP into the DH of P6 $Ret^{Ert2/+}$ pups and treating them with a low dosage of tamoxifen (Figure 2G). Early RET+ dDH neurons can be categorized into five groups based on morphology: islet cells (29%), radial cells (22%), vertical cells (16%), inverted stalked cells (8%), and unclassified neurons (25%) (Figures 2H–I). Islet cells are predominantly inhibitory, while other morphologies have been associated with both excitatory and inhibitory phenotypes (Heinke et al., 2004; Todd, 2010). Taken together, our results reveal complex intrinsic firing properties and morphologies of the early RET+ dDH neurons, which are consistent with their DH inhibitory neuron identity.

Finally, to visualize the gross anatomy of RET+ dDH neurons, we generated a BAC transgenic line, $Gsx1^{Cre}$, which mediates recombination predominately in the dorsal spinal cord and hindbrain beginning around E13.5 (Figures S3G–J). This is necessary because *Ret* is also expressed in primary somatosensory neurons, ventral horn interneurons, and motor neurons (Luo et al., 2007). We crossed the $Gsx1^{Cre}$ line with a $Ret^{CFP(f)}$ allele, in which CFP is expressed from the *Ret* locus upon Cre mediated recombination (Uesaka et al., 2008). Consistent with our *in situ* data, 1pw CFP+ DH neurons are located in spinal cord layers III through V, which is ventral to CGRP+ and IB4+ layers (central terminals of C nociceptors) and directly apposed to VGLUT1+ puncta (Figures 2J–K). High magnification images reveal that VGLUT1+ puncta, which mark presynaptic terminals of myelinated fibers including Aβ mechanoreceptors, are in close contact with CFP+ neurites. This suggests that early RET+ dDH neurons may receive direct synaptic inputs from Aβ mechanoreceptors (Figure 2L).

RET+ dDH Neurons Receive Excitatory Inputs from Aβ Mechanosensory Primary Afferents

To examine primary afferent inputs onto early RET+ dDH neurons, we prepared dorsal root attached horizontal or sagittal lumbar spinal cord slices from 4–5pw $Ret^{CFP/+}$ mice and performed whole cell patch clamp recording of CFP+ dDH neurons (Figure 3A). Upon electrical stimulation with an Aβ fiber intensity (8–26 pA) (Nakatsuka et al., 2000; Torsney and MacDermott, 2006), 35.2% (12/34) of the recorded neurons showed Aβ fiber-evoked

EPSCs. Mono or polysynaptic responses were further distinguished by 20 Hz stimulation (Figures 3B–C, and F); half of Aβ responsive neurons showed monosynaptic responses, while the remaining half displayed polysynaptic responses. In addition, 23.5% (8/34) of the recorded neurons showed evoked EPSCs upon stimulation with an Aδ fiber intensity (25–82 pA). With 10 Hz stimulation, we observed that 3/8 Aδ responsive neurons showed monosynaptic responses and the remaining showed polysynaptic responses (Figures 3D–F).

Since many afferent branches were disconnected during slice preparation, and since Aβ fibers from adjacent dorsal roots also innervate the examined spinal level (Brown, 1981; Niu et al., 2013) (Figure 3N), we speculated that 35.2% is an under estimation of Aβ inputs. To test this idea, we generated *Vglut1*^{Cre}*; Rosa*$^{ChR2(f)/+}$*; Ret*$^{CFP/+}$ mice, in which a blue light-activated cation channel, channelrhodopsin (ChR2) (Boyden et al., 2005), is specifically expressed in all VGLUT1+ neurons, including Aβ fibers (Figures S4A–F). With this method, we found 87.6 % (14/16) of recorded RET+ dDH neurons displaying light induced EPSCs ($EPSC_{LS}$) (Figures S4G–H). However, since *Vglut1* is also expressed in proprioceptors and corticospinal neurons, 87.6 % may be an over estimation. Finally, we used *Split*^{Cre} mice, which mainly mediate recombination in Aβ mechanoreceptors (Rutlin et al., 2014) but not corticospinal neurons in young adult mice (Figures S4I–O). We generated *Split*^{Cre}*; Rosa*$^{Tdt(f)/+}$*; Ret*$^{CFP/+}$ mice, in which Aβ mechanoreceptors are labeled with Td while RET+ dDH neurons are labeled with CFP. We found that ~70% of RET+ dDH neurons are in direct contact with Tdt+/VGLUT1+ puncta (Figures 3G–H). Moreover, we recorded Aβ inputs to RET+ dDH neurons using *Split*^{Cre}*; Rosa*$^{ChR2(f)/(f)}$*; Ret*$^{CFP/+}$ mice (Figures 3I and S4P). 80 % (16/20) of recorded neurons showed $EPSC_{LS}$. 13/16 of neurons were monosynaptic and the remaining neurons were polysynaptic (Figures 3J–M). Taken all into consideration, our results indicate that the majority of the RET+ dDH neurons are innervated by Aβ primary afferents.

RET+ dDH Neurons Receive Excitatory Inputs from C Nociceptive Primary Afferents

Given that some RET+ dDH neurons project to superficial spinal cord DH layers (Fig. 2H) and some C fibers innervate DH deep layers, RET+ dDH neurons may also receive C afferent inputs. We recorded evoked EPSCs from CFP+ dDH neurons of 4pw *Ret*$^{CFP/+}$ mice using C fiber intensity (>180pA) dorsal root electrical stimulation. Half (17/34) of recorded neurons showed C fiber induced EPSCs upon electrical stimulation: 14/17 of neurons received monosynaptic inputs, while 3/17 of neurons received polysynaptic inputs (Figure 4A–C).

C fiber nociceptors can be categorized into peptidergic and non-peptidergic subsets based on molecular marker expression and central/peripheral innervation (Zylka et al., 2005). Thus, we also conducted whole cell recording upon C fiber subtype specific stimulation. We generated *MrgD*$^{Ert2/+}$*; Rosa*$^{ChR2(f)/+}$*; Ret*$^{CFP/+}$ mice, in which ChR2 is specifically expressed in non-peptidergic primary afferents (Figures S5A–F). Half (12/24) of the recorded RET+ dDH neurons showed light-induced $EPSC_{LS}$. Twenty five percent (3/12) of these neurons received monosynaptic inputs and 9/12 of neurons received polysynaptic inputs (Figures 4D–F). These light-induced $EPSC_{LS}$ were also blocked by application of NBQX (Figure S5G). To specifically stimulate peptidergic fibers, we applied capsaicin, a TRPV1agonist,

onto $Ret^{CFP/+}$ spinal cord slices. The frequency of miniature EPSCs increased dramatically in half (9/18) of the recorded neurons, but the miniature EPSC amplitude and the resting membrane potential were not changed (Figures 4G–I and data not shown). Taken together, our results indicate that about half of RET+ dDH neurons receive C inputs, which include both peptidergic and non-peptidergic nociceptive primary afferents. Given the percentage of the RET+ dDH neurons receiving Aβ (~80%) or C (~50%) inputs, some of them must receive convergent inputs from different modality of afferents (see an example in Figure 4M). Indeed, based on electrical stimulation, 8.8%, 14.7%, 23.5% of recorded neurons received Aβ, Aδ, C inputs only, while 29.4 % of recorded neurons received two or three convergent inputs.

RET+ dDH Neurons Receive Polysynaptic Inhibitory Inputs from A and C Primary Afferents

Interestingly, some RET+ dDH neurons, which displayed excitatory monosynaptic Aβ or C inputs (Figures 4J and M), also received polysynaptic inhibitory inputs upon dorsal root stimulation of Aβ (Figures 4K–L) or C intensity (Figures 4N–O). These inhibitory inputs were blocked by the glycine receptor antagonist strychnine, but not by the $GABA_A$ receptor antagonist bicuculline. Given the polysynaptic nature of these IPSCs and that electrical C intensity stimuli also activate A fibers, we asked whether C afferents can truly inhibit RET+ dDH neurons. To answer this question, we conducted recordings with spinal cord slices of 3–5pw $MrgD^{Ert2/+}; Rosa^{ChR2(f)/+}; Ret^{CFP/+}$ mice, in which C afferents can be specifically activated by light. We found examples of RET+ dDH neurons that received both excitatory monosynaptic Aβ inputs and polysynaptic inhibitory C inputs. These inhibitory inputs were also blocked by strychnine but not by bicuculline (Figures 4P and Q). Taken together, our results suggest that RET+ dDH neurons receive not only excitatory but also polysynaptic inhibitory inputs from touch (Aβ) and pain (C) fibers (Figure 4R).

Early RET+ dDH Neurons Receive Inhibitory Inputs from Other Early RET+ dDH Neurons

We next sought to determine the downstream targets of early RET+ dDH neurons. We injected a Cre-dependent ChR2 virus (AAV1-Flex-ChR2-XFP, XFP is EYFP or mCherry) into one side of the lumbar dorsal spinal cord of P6 $Ret^{Ert2/+}$ mice, and then treated with tamoxifen for three days (Figure 5A). AAV1 was first used because a previous study suggested that it has a low retrograde infection rate (Foster et al., 2015). As expected, we found ChR2+ cell bodies and neurites in the dDH, which were ventral to the CGRP+ and IB4+ layers (Figure 5B). Nevertheless, we also noticed some ChR2+ neurons in the ipsilateral L4 and L5 DRGs (data not shown), which was due to the retrograde infection of the RET+ DRG neurons (Luo et al., 2007). Since the primary afferents are excitatory while the early RET+ dDH neurons are inhibitory, their postsynaptic responses could be readily differentiated during physiological recordings. We therefore tolerated this modest retrograde infection for our monosynaptic physiological recording experiments. To confirm ChR2 function in the labeled DH neurons, we performed whole cell recording on ChR2+ neurons. They displayed light-evoked currents with a reversal potential around 0 mV (Figure 5C) and showed light-evoked action potentials that faithfully followed light stimulation (up to 50Hz) (Figure 5D). These data suggest that ChR2 functions as expected in early RET+ dDH neurons. Interestingly, we found that the majority (86.7 % (13/15), Figure 5F) of ChR2+ neurons also display monosynaptic light-evoked IPSCs (~2 ms delay upon light stimulation)

when held at the reversal potential of the ChR2 channel. These IPSCs were blocked by strychnine and by the sodium channel blocker tetrodotoxin (TTX), but not by bicuculline (Figure 5E). This result demonstrates that early RET+ dDH neurons make extensive inhibitory synapses onto other early RET+ dDH neurons, and that this inter-cellular communication is mainly mediated by glycine.

Early RET+ dDH Neurons Inhibit DH Pain and Touch Pathways

Next, we recorded from ChR2 negative DH neurons in layers II and III upon light stimulation. 83.9 % (26/31) of the recorded neurons, the cell bodies of which are surrounded by ChR2+ fibers, displayed light-evoked monosynaptic $IPSC_L$s (Figures 5G–H). Most of these responses were also blocked by strychnine (data not shown). To determine the molecular identity of ChR2 negative responsive cells, we focused on PKCγ+ excitatory interneurons that transmit Aβ/Aδ touch information to projection neurons (Lu et al., 2013) and SST+ excitatory interneurons that mainly mediate C fiber mechanical pain sensation (Duan et al., 2014). ChR2+ neurites surround PKCγ+ and SST+ neurons (Figures 5I–J), suggesting that early RET+ dDH neurons might directly synapse onto these excitatory interneurons. Indeed, when we performed single cell RT-PCR for *Pkcγ* or *Sst* (Figure 5K–L) with responsive neurons, we found 29.4 % (5/17) of them were PKCγ+, 38.9% (7/18) were SST+, but none were Dyn+ (data not shown). Taken together, our data indicate that early RET+ neurons directly inhibit PKCγ+ and SST+ excitatory interneurons, through which they can negatively regulate DH transmission of touch and pain pathways (Figure 5O).

We also observed that early RET+ dDH neurons make presynaptic inhibitory synapses onto DH primary afferent terminals. Although presynaptic inhibitory terminals around motor neurons contain GAD65 but not GAD67 (Fink et al., 2014), both GAD65 and GAD67 appear to mark presynaptic inhibitory terminals in the spinal cord DH (Figures S5H–L). We co-stained both GADs with mCherry, which marks the neurites of inhibitory early RET+ dDH neurons, and with VGLUT1, which marks the presynaptic terminals of Aβ fibers (Figure S5M). We found that GAD+/mCherry+ puncta are in close proximity to VGLUT1+ puncta in the DH, suggesting that early RET+ dDH neurons could inhibit Aβ fibers presynaptically. Moreover, we combined electrical stimulation to activate primary afferents and optical stimulation to activate early RET+ dDH neurons using spinal cord slices of 3 to 4 pw $Ret^{Ert2/+}$; *AAV8-Flex-ChR2* mice. AAV8 was used for the remaining experiments to preferentially infect spinal cord DH neurons (Figures S6A–C), consistent with a recent publication (Peirs et al., 2015). We identified layer I–II ChR2 negative DH neurons receiving no postsynaptic inputs from ChR2+ neurites and recorded electrically simulated paired pulse responses (PPR) before and after blue laser stimulation (1 second 20 Hz light stimulation, 0.1 ms pulses). The paired pulse stimulation caused a depression of the second response compared to the first response (Figures 5M–N). Interestingly, the optical stimulation inhibited the first response but increased the second one (Figures 5M–N), suggesting that activation of early RET+ dDH neurons prevents the depletion of presynaptic vesicles upon the first electrical stimulation. Since the recorded neurons did not receive direct $IPSC_{LS}$ from early RET+ dDH neurons, this effect must be mediated by presynaptic inhibition. This presynaptic inhibition was blocked by the $GABA_B$ receptor antagonist, CGP55845, but not by strychnine (Figure S5N and data not shown), suggesting that GABA but not glycine is

used by early RET+ dDH neurons for presynaptic inhibition. Together, our results show that early RET+ dDH neurons negatively regulate DH transmission of touch and pain pathways through both pre- and postsynaptic mechanisms (Figure 5O).

Activation of Early RET+ dDH Neurons Reverses Hyperactivity of Aβ and C Pathways upon Dis-inhibition

Spinal cord DH dis-inhibition leads to hyperactivity and aberrant transmission of touch and pain pathways, which is considered to be an important mechanism underlying hyperalgesia and/or allodynia (Torsney and MacDermott, 2006). We next tested whether activation of early RET+ dDH neurons can reverse some of this hyperactivity and aberrant transmission. In the spinal cord slices of 3 to 4 pw $Ret^{Ert2/+}$; *AAV8-Flex-ChR2* mice, we recorded primary afferent-triggered responses from ChR2 negative DH neurons upon pharmacological dis-inhibition, and compared their responses before and after light stimulation (Figure 6A). With application of bicuculline and/or strychnine, layer I to IIm DH neurons showed strong polysynaptic Aβ responses (Figure 6B). Remarkably, activation of early RET+ dDH neurons significantly blocked this dis-inhibition in 3/6 of the superficial DH neurons we examined (Figure 6C). Similarly, we saw an increase in C intensity triggered polysynaptic responses upon application of bicuculline and/or strychnine (Figure 6D), which could be induced from all types of primary afferents including C fibers. This hyperactivity was inhibited by activation of early RET+ dDH neurons in 3/7 examined neurons as well (Figure 6E). Further pharmacological characterization suggested that early RET+ dDH neurons executed this inhibition through $GABA_B$ receptors (Figure S5O), which could be through either pre- and/or postsynaptic inhibition. Collectively, our results suggest that early RET+ dDH neurons play critical roles in negatively modulating both pain and touch DH pathways.

Specific Ablation of Early RET+ dDH Neurons

To test the functions of early RET+ dDH neurons in pain behaviors, we injected a Cre-dependent virus expressing diphtheria toxin (AAV8-Flex-DTA)) (Wu et al., 2014) into one side of the DH of P6 $Ret^{Ert2/+}$ mice and treated them with tamoxifen at P7–9 to ablate the early RET+ dDH neurons (DTA Abl mice, Figure 6F). We used two types of controls (Table S1): wild type littermates injected with AAV8-Flex-DTA (control 1) or $Ret^{Ert2/+}$ mice injected with AAV8-Flex-TurboRed (control 2). To quantify the ablation efficiency, we also crossed $Ret^{Ert2/+}$ mice with a $Tau^{nlacZ(f)}$ reporter allele to genetically label early Ret+ dDH neurons with a nuclear LacZ. Many LacZ+ neurons were present in the DH of control 2 mice or in the contralateral side of DTA Abl mice (Figures 6G–H). However, the number of LacZ+ neurons was significantly reduced in the ipsilateral DH of DTA Abl mice (Figures 6I–J). Consistently, GAD1/2+ neurons in dDH show ~18% reduction (Figures S6D–E). To determine if RET+ lumbar DRG neurons were ablated by AAV8-Flex-DTA through retrograde infection, we quantified the number of RET+ neurons in ipsilateral L3–L5 DRGs of DTA Abl and control 2 mice. We found no significant difference in the number of RET+/NF200+ DRG neurons (Figures 6K–M), most of which are Aβ rapidly adapting low-threshold mechanoreceptors (Luo et al., 2009), or the number of RET+/NF200− DRG neurons, most of which are C fiber non-peptidergic nociceptors (Luo et al., 2007). Taken together, our results demonstrate that injection of conditional DTA virus into the $Ret^{Ert2/+}$ mouse DH can specifically ablate early RET+ dDH neurons.

To determine if the overall spinal cord structure was altered upon surgery and virus injection, we conducted immunostaining and *in situ* hybridization with a panel of spinal cord markers (Figures S6D–M and S7). No obvious changes in the DH laminar structure were found between control and DTA Abl mice, based on *in situ* hybridization of *Gad1/2*, *Glyt2*, *Vglut2*, *Dyn*, and *Sst* (Figures S6D–M), staining of VGLUT1, CGRP, IB4, and PKCγ (Figures S7A–H), and cresyl-violet staining (Figures S7I–J). Moreover, we determined whether viral infection and neuronal cell death induced activation of DH microglia and astrocytes. No marked upregulation of the microglia marker Iba-1 or the astrocyte marker GFAP was found in adult control and DTA Abl mouse DH (Figures S7K–N). These findings demonstrate that the spinal cord structure of the DTA Abl mice is roughly normal.

Loss of Early RET+ dDH Neurons Leads to Abnormal Acute Pain Sensation

Consistent with our histological observations indicating the integrity of the DTA Abl lumbar spinal cord, post operational adult mice displayed normal walking and daily behaviors. No significant difference was seen when motor behaviors of control and DTA Abl mice were further examined (Table S2).

Next, we tested these mice using a battery of pain-related behavioral assays. Both male and female adult DTA Abl mice displayed static and dynamic mechanical allodynia, indicated by significant increases in paw withdrawal frequency (Figures 7A and S8A) and in dynamic allodynia score (Figures 7B and S8B) on the ipsilateral but not contralateral side, when compared to both control groups. We then examined noxious stimulation-evoked hyperalgesia, which is mediated mainly by C- and Aδ-fibers (Sandkuhler, 2009), in control and DTA Abl mice. Compared to the two control groups, we observed a significant increase in paw withdrawal duration in response to a safety pin (Figures 7C and S8C) and a marked reduction in paw withdrawal latency in response to radiant heat/cold plate on the ipsilateral side of male and female adult DTA Abl mice (Figures 7D–E, and S8D–E), indicating that DTA Abl mice display mechanical, thermal, and cold hyperalgesia. In addition, the duration of licking and/or lifting upon hind paw injection of capsaicin, which is used as readout of feeling pain, was much longer in adult DTA Abl mice than either of the two control groups (Figures 7F and S8F). This further supports that a specific loss of early RET+ dDH neurons leads to more pain sensation upon noxious stimulation.

In addition to the evoked responses, we tested stimulus-independent spontaneous pain by adopting a conditional place preference paradigm (He et al., 2012). This paradigm relies on the fact that analgesic agents (e.g., lidocaine), which are not rewarding in the absence of pain, should become rewarding in the presence of spontaneous/ongoing pain. After three trials of pairing, male or female adult DTA Abl mice exhibited an obvious preference (i.e. spent more time) toward the lidocaine-paired chamber, whereas both groups of control mice displayed no preference for either chamber (Figures 7G and S8G). This finding suggests that DTA Abl mice experience spontaneous pain.

Given that early RET+ dDH neurons release both GABA and glycine (Figures 1D–E, 5E, and S5N–O), it is possible that behavioral changes in DTA Abl mice may be attributed to a loss of GABA and/or glycine synaptic transmission. Indeed, intrathecal administration of gabapentin (a structural analog of GABA) or glycine greatly blocked static mechanical

allodynia in adult DTA Abl mice. Moreover, this block was reversed by co-administration of bicuculline and CGP55845, or strychnine (Figures 7H–I, and S8H–I). Therefore, early RET + dDH neurons gate mechanical allodynia through both GABAergic and glycinergic transmission in the spinal cord DH.

Loss of Early RET+ dDH Neurons Leads to More Severe Inflammatory and Neuropathic Pain

A fundamental feature of inflammatory and neuropathic pain is hypersensitivity in response to somatosensory stimulation. We next asked whether the hypersensitive responses seen in inflammatory and neuropathic pain models are exacerbated upon a loss of early RET+ dDH inhibitory interneurons. To model inflammatory pain, formalin or complete Freund's adjuvant (CFA) were injected into the plantar side of the ipsilateral hind paw of control and DTA Abl mice. Formalin injection typically produces two phases of nociceptive behaviors (e.g., flinches and shakes) during a one-hour observation period (Ma and Woolf, 1996; Tjolsen et al., 1992). DTA Abl male and female mice showed significant increases in the number of flinches and shakes during both phases compared to the control groups (Figures 7J–K, and S8J–K). In addition, CFA injection leaded to a long-lasting inflammatory static mechanical allodynia and thermal hyperalgesia on the injected side (Park et al., 2009). Compared to both control groups, DTA Abl mice showed a significantly higher magnitude and a markedly prolonged duration of CFA-induced static mechanical allodynia and thermal hyperalgesia responses (Figures 7L–M, and S8L–M). To model neuropathic pain, unilateral lumbar fourth (L4) spinal nerve ligation (SNL) was carried out in control and DTA Abl mice. Similar to the CFA injection, SNL produces a long-lasting static mechanical allodynia and thermal hyperalgesia. Compared to the controls, DTA Abl male and female mice exhibited an even higher magnitude of SNL-induced static mechanical allodynia and thermal hyperalgesia responses, as well as a dramatically prolonged duration of SNL-induced mechanical allodynia response (Figure 7N–O, and S8N–O). Taken together, our data suggest that mice experience more severe inflammatory and neuropathic pain upon ablation of early RET+ dDH neurons.

Acute Activation of Early RET+ dDH Neurons Reduces Basal Pain Perception and Relieves Inflammatory and Neuropathic Pain

Finally, we adopted a strategy utilizing DREADDs (Designer Receptors Exclusively Activated by Designer Drugs) (Dong et al., 2010) to determine whether acute activation of early RET+ dDH neurons would affect basal pain perception and CFA- or SNL-induced hypersensitive responses. We unilaterally injected AAV8-hSyn-DIO-hM3D(Gq)-mCherry into the L4/5 DH of Ret^{Ert2} mice to specifically express hM3Dq-mCherry in early RET+ dDH neurons (hM3Dq mice; Figure 8A). The mCherry+ (but not negative) neurons were activated by the receptor-specific ligand, clozapine-n-oxide (CNO) (Figure 8B). Upon intraperitoneal CNO injection (Table S3), hM3Dq mice showed a significant reduction in paw withdrawal frequency in response to mechanical stimulation and an increase in paw withdrawal latency in response to thermal stimulation compared to control mice (Figures 8C–D), suggesting that acute activation of early RET+ dDH neurons decreases basal pain perception. Furthermore, upon CNO injection, hM3Dq mice displayed attenuations of CFA-induced increases in paw withdrawal frequency and CFA-induced decreases in paw

withdrawal latency on days 1 and 3 post-CFA (Figures 8E–F). Similar phenomena were observed in the hM3Dq mice on days 7 and 14 post-SNL (Figures 8G–H). In contrast, all control mice exhibited robust CFA- or SNL-induced increases in paw withdrawal frequency and decrease in paw withdrawal latency (Figure 8E–8H). Collectively, these findings indicate that acute activation of early RET+ dDH neurons inhibits acute and chronic pain.

Discussion

In summary, we have identified a molecularly defined population of spinal cord neurons, the early RET+ dDH neurons, which play critical roles in mediating crosstalk between pain and touch pathways. These early RET+ dDH neurons are inhibitory interneurons and receive excitatory as well as polysynaptic inhibitory inputs from touch and pain afferents. Interestingly, most RET+ dDH neurons inhibit each other, and thus could serve as an inhibitory switch between pain and touch pathways. Moreover, early RET+ dDH neurons directly inhibit PKCγ+ or SST+ excitatory interneurons postsynaptically and primary afferents presynaptically. Finally, specific ablation of the early RET+ dDH neurons induces acute pain and augments chronic pain, whereas acute activation of these neurons reduces basal pain perception and attenuates chronic pain. Taken together, we propose a model in which some early RET+ dDH neurons act as gating neurons to modulate pain transmission in the spinal cord (Figure 8I).

Early RET+ dDH Neurons Are a New Functional Class of Spinal Cord Inhibitory Interneurons

DH inhibitory interneurons, which utilize GABA and/or glycine as neurotransmitters, play critical roles in modulating somatosensation. They have complicated morphologies and firing patterns (Heinke et al., 2004; Todd, 2010), which makes the task of defining functional subpopulations of spinal cord inhibitory interneurons challenging. Here, we identified a novel population of DH interneurons located in the deep layers III through V of the spinal cord, which express *Ret* neonatally. Their molecular profiles, morphologies, neurochemical expression, and intrinsic firing patterns suggest that they are inhibitory interneurons (Figures 1–2, and S2). Early RET+ dDH neurons make up one third of the total inhibitory interneurons in layers III through V and overlap ~50% with *Glyt2*+, ~80% with *Gad*1/2+, and 25% to 30% with PV+ DH neurons, but not with other known DH inhibitory neuron markers, nNOS and Dyn. Thus, early RET+ dDH neurons comprise a new population of spinal cord inhibitory interneurons. Interestingly, our results suggest that RET+ dDH neurons mainly use glycine to communicate with other DH neurons (Figure 5E and data not shown) but use GABA to communicate with primary afferents (Figure S5N). Our results also suggest that $GABA_B$ receptors play important functions in presynaptic inhibition of superficial DH neurons (Figures 5M–N and S5N), which is consistent with their high expression in primary afferents and previous functional studies (Chery and De Koninck, 2000; Towers et al., 2000; Yang and Ma, 2011). Nevertheless, our results do not exclude a contribution of $GABA_A$ receptors in presynaptic inhibition. Since most superficial layer neurons show polysynaptic events upon bicuculline treatment in our hands (“dis-inhibition”, see Figures 6B and 6D for examples, and (Torsney and MacDermott, 2006)), it is difficult for us to determine and compare the peak currents of monosynaptic responses with or

without bicuculline treatment. Thus, we could not determine the contribution of $GABA_A$ receptors (Guo and Hu, 2014; Paul et al., 2012) in this regard. In short, given that most previously characterized classes of DH inhibitory interneurons are located in more superficial DH layers (Lu and Perl, 2003; Todd, 2010; Yasaka et al., 2010), our results provide novel insight into the circuits and functions of deep layer DH inhibitory interneurons.

Neural Circuits Mediating Cross Talk between Pain and Touch Pathways

Crosstalk between touch and pain pathways (the “gate control theory” of pain) was proposed by Melzack and Wall a half century ago (Figure 1A, (Melzack and Wall, 1965)) and is widely used to explain pain-related phenomena. However, the neural substrates underlying the GCT have remained largely elusive. A series of recent studies have characterized the circuitry and function of several molecularly defined populations of DH interneurons in mediating and modulating touch and pain sensation, including PKCγ+, RORα+, VGLUT3+, and somatostatin (SST)+ excitatory interneurons, and Dyn+, PV+, TRPV1+, and GLYT2+ inhibitory interneurons(Bourane, 2015; Duan et al., 2014; Foster et al., 2015; Kim et al., 2012; Lu et al., 2013; Peirs et al., 2015; Petitjean et al., 2015). Despite these studies, the neural circuits underlying some aspects of the GCT remain puzzling. How does activation of nociceptive C fibers inhibit “gating neurons” and thus open the “gate” for transmitting both pain and touch information? Since primary C afferents are excitatory, they must dis-inhibit the “gating” neurons through some inhibitory interneurons.

Here we found that early RET+ dDH neurons exhibit interesting circuit properties, through which they could play a role in the GCT gate. Early RET+ dDH neurons can be categorized into two groups based on excitatory afferent inputs: those that receive C only or C and A inputs (“C type”), and those that receive A only inputs (“A type”) (Figures 3 and 4). In addition, early RET+ dDH neurons negatively regulate both touch and pain DH pathways by inhibiting PKCγ+ and SST+ excitatory interneurons as well as primary afferents (Figure 5). Thus, some RET+ dDH neurons, likely the “A type”, receiving excitatory A inputs and inhibiting transmission of both pain and touch pathways, serve as “gating” neurons. Interestingly, early RET+ dDH neurons also receive polysynaptic glycinergic inhibitory inputs from A and C afferents (Figure 4). Since the majority of early RET+ dDH neurons receive glycinergic inhibitory inputs from other early RET+ dDH neurons (Figures 5E–F), we speculate that some antagonization between C and A pathways might be mediated by early RET+ dDH neurons themselves (Figure 8I). It seems possible that C afferents dis-inhibit the “A type” early RET+ dDH neurons through the “C type” early RET+ dDH neurons or other DH inhibitory neurons and thus open the “gate”. Collectively, our results suggest that early RET+ dDH neurons play a critical function in mediating crosstalk between touch and pain pathways.

Nevertheless, early RET+ dDH neurons likely are not the only “gating” neurons. Dyn+ DH inhibitory neurons, which are located in DH superficial layers, are another population of “gating” neurons (Duan et al., 2014). We found that the early RET+ dDH neurons and Dyn+ DH neurons are well segregated in different DH layers (Figure. S1). In addition, the early RET+ dDH neurons don’t seem to directly inhibit Dyn+ neurons based on our recordings

and single cell RT-PCR (data not shown), suggesting that they likely function in parallel pathways. Since some Dyn+ neurons also receive C inputs, it remains to be determined whether Dyn+ neurons could inhibit “A type” early RET+ dDH neurons. In short, multiple types of “gating” neurons may exist to mediate antagonization between touch and pain pathways.

Early RET+ dDH Neurons Modulate Pain Sensation

DH inhibitory interneurons play critical roles in modulating pain sensation (Sivilotti and Woolf, 1994) and are important drug targets for treating pain. However, the antagonists that target large swathes of inhibitory interneurons are too broad and likely yield unwanted side effects. Thus, identification of subpopulations of DH inhibitory interneurons, which play critical roles in the modulation of pain sensation, may provide more specific drug targeting options. Our data suggest that early RET+ dDH neurons play important roles in modulating both acute and chronic pain. We found that early RET+ dDH neurons directly inhibit DH A and C pathways through both pre- and postsynaptic inhibition (Figure 5). In addition, activation of early RET+ dDH neurons blocks the hyperactivity induced by pharmacological dis-inhibition (Figures 6B–E). Since spinal cord DH dis-inhibition is considered to be an important mechanism underlying chronic pain, early RET+ dDH neurons could be important players in both acute and chronic pain conditions. Indeed, we found direct evidence that early RET+ dDH neurons play critical roles in acute and chronic pain sensation using behavior assays (Figures 7, 8, S7, and S8). Loss of early RET+ dDH neurons leads to pain hypersensitivity, mechanical allodynia, spontaneous pain, and more severe pain phenotypes in inflammatory and neuropathic pain models. On the other hand, acute activation of these neurons reduces basal pain perception and relieves inflammatory and neuropathic pain. Collectively, our results reveal that early RET+ dDH neurons contribute to inflammatory and neuropathic pain genesis and that blocking their activities may have clinical applications in chronic pain management.

Experimental Procedures

Mouse lines and treatments

Mice used for molecular characterization and physiological recordings were raised in facilities at the University of Pennsylvania. Those used for behavior studies were housed at the Rutgers New Jersey Medical School. All animal treatments were conducted in accordance with protocols approved by the Institutional Animal Care and Use Committee and the National Institutes of Health guidelines. Information regarding mouse lines and details of experimental procedures are described in the Supplemental Information.

Immunohistochemistry, *In Situ* Hybridization, and Image Analysis

Immunohistochemistry, *in situ* hybridization, and image analysis are similar to those previously described (Fleming et al., 2015; Niu et al., 2013; Niu et al., 2014). The detailed experimental procedures are described in the Supplemental Experimental Procedures.

Electrophysiology and Optogenetics

Whole cell patch clamp recording with transverse or sagittal spinal cord sections and dorsal root stimulation were performed as previously described (Torsney and MacDermott, 2006). ChR2 was activated using a 473nm blue laser (FTEC2473V65-YF0, Blue Sky Research, Milpitas). Details are described in the Supplemental Experimental Procedures.

Virus Production and Injections

AAV viruses were purchased from either the University of Pennsylvania or University of North Carolina Viral Vector Core. Details about the intraspinal virus injections are described in the Supplemental Experimental Procedures.

Behavior Assays and Statistics

Locomotor and somatosensory behaviors were tested as previously described (Bourane et al., 2015; Duan et al., 2014; Xu et al., 2014). See details in the Supplemental Experimental Procedures. Student's t test, one-way or two-way ANOVA followed by Tukey post hoc analysis were used where appropriate.

Supplementary Material

Refer to Web version on PubMed Central for supplementary material.

Acknowledgments

We thank Dr. Qin Liu at Washington University in St. Louis and other Luo and Tao lab members for helpful comments on the manuscript. We thank the Penn transgenic core for injecting the $GSX1^{Cre}$ BAC. We thank the Penn and UNC vector core and Dr. Naoshige Uchida at Harvard University for providing different viruses. We thank Drs. Tom Jessell and Noga Vardi for sharing anti-GAD1 and 2 antibodies. This work was supported by National Institutes of Health (NIH) grant (NS083702) and the Klingenstein-Simons Fellowship Award in the Neurosciences to W.L., by NIH grant (NS092297) to W.O., by NIH grant (NS086168) to M.F. and by NIH grants (NS072206, NS NS094664, DA033390, and HL117684) to Y.-X.T.

References

Abraira VE, Ginty DD. The sensory neurons of touch. Neuron. 2013; 79:618–639. [PubMed: 23972592]

Bardoni R, Takazawa T, Tong CKK, Choudhury P, Scherrer G, Macdermott AB. Pre- and postsynaptic inhibitory control in the spinal cord dorsal horn. Annals of the New York Academy of Sciences. 2013; 1279:90–96. [PubMed: 23531006]

Basbaum AI, Bautista DM, Scherrer G, Julius D. Cellular and molecular mechanisms of pain. Cell. 2009; 139:267–284. [PubMed: 19837031]

Bourane S, G KS, Britz O, Dalet A, Barrio MGD, Stam FJ, Garcia-Campmany L, Koch S, Goulding M. Identification of a Spinal Circuit for Light Touch and Fine Motor Control. Cell. 2015; 160

Boyden ES, Zhang F, Bamberg E, Nagel G, Deisseroth K. Millisecond-timescale, genetically targeted optical control of neural activity. Nat Neurosci. 2005; 8:1263–1268. [PubMed: 16116447]

Brown, AG., editor. Organization in the Spinal Cord. Berlin Heidelberg New York: Springer-Verlag; 1981.

Campbell JN, Raja SN, Meyer RA, Mackinnon SE. Myelinated afferents signal the hyperalgesia associated with nerve injury. Pain. 1988; 32:89–94. [PubMed: 3340426]

Chery N, De Koninck Y. GABA(B) receptors are the first target of released GABA at lamina I inhibitory synapses in the adult rat spinal cord. J Neurophysiol. 2000; 84:1006–1011. [PubMed: 10938323]

Dong S, Rogan SC, Roth BL. Directed molecular evolution of DREADDs: a generic approach to creating next-generation RASSLs. Nat Protoc. 2010; 5:561–573. [PubMed: 20203671]

Duan B, Cheng L, Bourane S, Britz O, Padilla C, Garcia-Campmany L, Krashes M, Knowlton W, Velasquez T, Ren X, et al. Identification of spinal circuits transmitting and gating mechanical pain. Cell. 2014; 159:1417–1432. [PubMed: 25467445]

Fink AJ, Croce KR, Huang ZJ, Abbott LF, Jessell TM, Azim E. Presynaptic inhibition of spinal sensory feedback ensures smooth movement. Nature. 2014; 509:43–48. [PubMed: 24784215]

Fleming MS, Luo W. The anatomy, function, and development of mammalian Aβ low-threshold mechanoreceptors. Frontiers in biology. 2013; 8

Foster E, Wildner H, Tudeau L, Haueter S, Ralvenius WT, Jegen M, Johannssen H, Hösli L, Haenraets K, Ghanem A. Targeted Ablation, Silencing, and Activation Establish Glycinergic Dorsal Horn Neurons as Key Components of a Spinal Gate for Pain and Itch. Neuron. 2015; 85:1289–1304. [PubMed: 25789756]

Guo D, Hu J. Spinal presynaptic inhibition in pain control. Neuroscience. 2014; 283:95–106. [PubMed: 25255936]

He Y, Tian X, Hu X, Porreca F, Wang ZJ. Negative reinforcement reveals non-evoked ongoing pain in mice with tissue or nerve injury. J Pain. 2012; 13:598–607. [PubMed: 22609247]

Heinke B, Ruscheweyh R, Forsthuber L, Wunderbaldinger G, Sandkühler J. Physiological, neurochemical and morphological properties of a subgroup of GABAergic spinal lamina II neurones identified by expression of green fluorescent protein in mice. The Journal of physiology. 2004; 560:249–266. [PubMed: 15284347]

Kim YH, Back SK, Davies AJ, Jeong H, Jo HJ, Chung G, Na HS, Bae YC, Kim SJ, Kim JS, et al. TRPV1 in GABAergic interneurons mediates neuropathic mechanical allodynia and disinhibition of the nociceptive circuitry in the spinal cord. Neuron. 2012; 74:640–647. [PubMed: 22632722]

Lu Y, Dong H, Gao Y, Gong Y, Ren Y, Gu N, Zhou S, Xia N, Sun YY, Ji RR, et al. A feed-forward spinal cord glycinergic neural circuit gates mechanical allodynia. J Clin Invest. 2013; 123:4050–4062. [PubMed: 23979158]

Lu Y, Perl ER. A specific inhibitory pathway between substantia gelatinosa neurons receiving direct C-fiber input. The Journal of neuroscience: the official journal of the Society for Neuroscience. 2003; 23:8752–8758. [PubMed: 14507975]

Luo W, Enomoto H, Rice FL, Milbrandt J, Ginty DD. Molecular identification of rapidly adapting mechanoreceptors and their developmental dependence on ret signaling. Neuron. 2009; 64:841–856. [PubMed: 20064391]

Luo W, Wickramasinghe SR, Savitt JM, Griffin JW, Dawson TM, Ginty DD. A hierarchical NGF signaling cascade controls Ret-dependent and Ret-independent events during development of nonpeptidergic DRG neurons. Neuron. 2007; 54:739–754. [PubMed: 17553423]

Ma Q. Population coding of somatic sensations. Neurosci Bull. 2012; 28:91–99. [PubMed: 22466120]

Ma QP, Woolf CJ. Progressive tactile hypersensitivity: an inflammation-induced incremental increase in the excitability of the spinal cord. Pain. 1996; 67:97–106. [PubMed: 8895236]

Melzack R, Wall PD. Pain mechanisms: a new theory. Science. 1965; 150:971–979. [PubMed: 5320816]

Nakatsuka T, Ataka T, Kumamoto E, Tamaki T, Yoshimura M. Alteration in synaptic inputs through C-afferent fibers to substantia gelatinosa neurons of the rat spinal dorsal horn during postnatal development. Neuroscience. 2000; 99:549–556. [PubMed: 11029546]

Niu J, Ding L, Li JJ, Kim H, Liu J, Li H, Moberly A, Badea TC, Duncan ID, Son YJJ, et al. Modality-based organization of ascending somatosensory axons in the direct dorsal column pathway. The Journal of neuroscience: the official journal of the Society for Neuroscience. 2013; 33:17691–17709. [PubMed: 24198362]

Park JS, Voitenko N, Petralia RS, Guan X, Xu JT, Steinberg JP, Takamiya K, Sotnik A, Kopach O, Huganir RL, et al. Persistent inflammation induces GluR2 internalization via NMDA receptor-triggered PKC activation in dorsal horn neurons. J Neurosci. 2009; 29:3206–3219. [PubMed: 19279258]

Paul J, Zeilhofer HU, Fritschy JM. Selective distribution of GABA(A) receptor subtypes in mouse spinal dorsal horn neurons and primary afferents. J Comp Neurol. 2012; 520:3895–3911. [PubMed: 22522945]

Peirs C, Williams SP, Zhao X, Walsh CE, Gedeon JY, Cagle NE, Goldring AC, Hioki H, Liu Z, Marell PS, et al. Dorsal Horn Circuits for Persistent Mechanical Pain. Neuron. 2015; 87:797–812. [PubMed: 26291162]

Petitjean H, Pawlowski SA, Fraine SL, Sharif B, Hamad D, Fatima T, Berg J, Brown CM, Jan LY, Ribeiro-da-Silva A, et al. Dorsal Horn Parvalbumin Neurons Are Gate-Keepers of Touch-Evoked Pain after Nerve Injury. Cell Rep. 2015; 13:1246–1257. [PubMed: 26527000]

Rutlin M, Ho CY, Abraira VE, Cassidy C, Bai L, Woodbury CJ, Ginty DD. The cellular and molecular basis of direction selectivity of Adelta-LTMRs. Cell. 2014; 159:1640–1651. [PubMed: 25525881]

Sandkuhler J. Models and mechanisms of hyperalgesia and allodynia. Physiol Rev. 2009; 89:707–758. [PubMed: 19342617]

Sivilotti L, Woolf CJ. The contribution of GABAA and glycine receptors to central sensitization: disinhibition and touch-evoked allodynia in the spinal cord. J Neurophysiol. 1994; 72:169–179. [PubMed: 7965003]

Tjolsen A, Berge OG, Hunskaar S, Rosland JH, Hole K. The formalin test: an evaluation of the method. PAIN. 1992; 51:5–17. [PubMed: 1454405]

Todd AJ. Neuronal circuitry for pain processing in the dorsal horn. Nature reviews Neuroscience. 2010; 11:823–836. [PubMed: 21068766]

Torsney C, MacDermott AB. Disinhibition opens the gate to pathological pain signaling in superficial neurokinin 1 receptor-expressing neurons in rat spinal cord. The Journal of neuroscience: the official journal of the Society for Neuroscience. 2006; 26:1833–1843. [PubMed: 16467532]

Towers S, Princivalle A, Billinton A, Edmunds M, Bettler B, Urban L, Castro-Lopes J, Bowery NG. GABAB receptor protein and mRNA distribution in rat spinal cord and dorsal root ganglia. Eur J Neurosci. 2000; 12:3201–3210. [PubMed: 10998104]

Truini A, Garcia-Larrea L, Cruccu G. Reappraising neuropathic pain in humans–how symptoms help disclose mechanisms. Nat Rev Neurol. 2013; 9:572–582. [PubMed: 24018479]

Uesaka T, Nagashimada M, Yonemura S, Enomoto H. Diminished Ret expression compromises neuronal survival in the colon and causes intestinal aganglionosis in mice. J Clin Invest. 2008; 118:1890–1898. [PubMed: 18414682]

Wu Z, Autry AE, Bergan JF, Watabe-Uchida M, Dulac CG. Galanin neurons in the medial preoptic area govern parental behaviour. Nature. 2014; 509:325–330. [PubMed: 24828191]

Yang K, Ma H. Blockade of GABA(B) receptors facilitates evoked neurotransmitter release at spinal dorsal horn synapse. Neuroscience. 2011; 193:411–420. [PubMed: 21807068]

Yasaka T, Tiong SY, Hughes DI, Riddell JS, Todd AJ. Populations of inhibitory and excitatory interneurons in lamina II of the adult rat spinal dorsal horn revealed by a combined electrophysiological and anatomical approach. Pain. 2010; 151:475–488. [PubMed: 20817353]

Zylka MJ, Rice FL, Anderson DJ. Topographically distinct epidermal nociceptive circuits revealed by axonal tracers targeted to Mrgprd. Neuron. 2005; 45:17–25. [PubMed: 15629699]

Highlights

- Early RET+ dDH neurons define a new population of DH inhibitory interneurons.
- Early RET+ dDH neurons mediate crosstalk between touch and pain pathways.
- Early RET+ dDH neurons inhibit DH transmission of both touch and pain pathways.
- Early RET+ dDH neurons play critical roles in acute and chronic pain sensation.

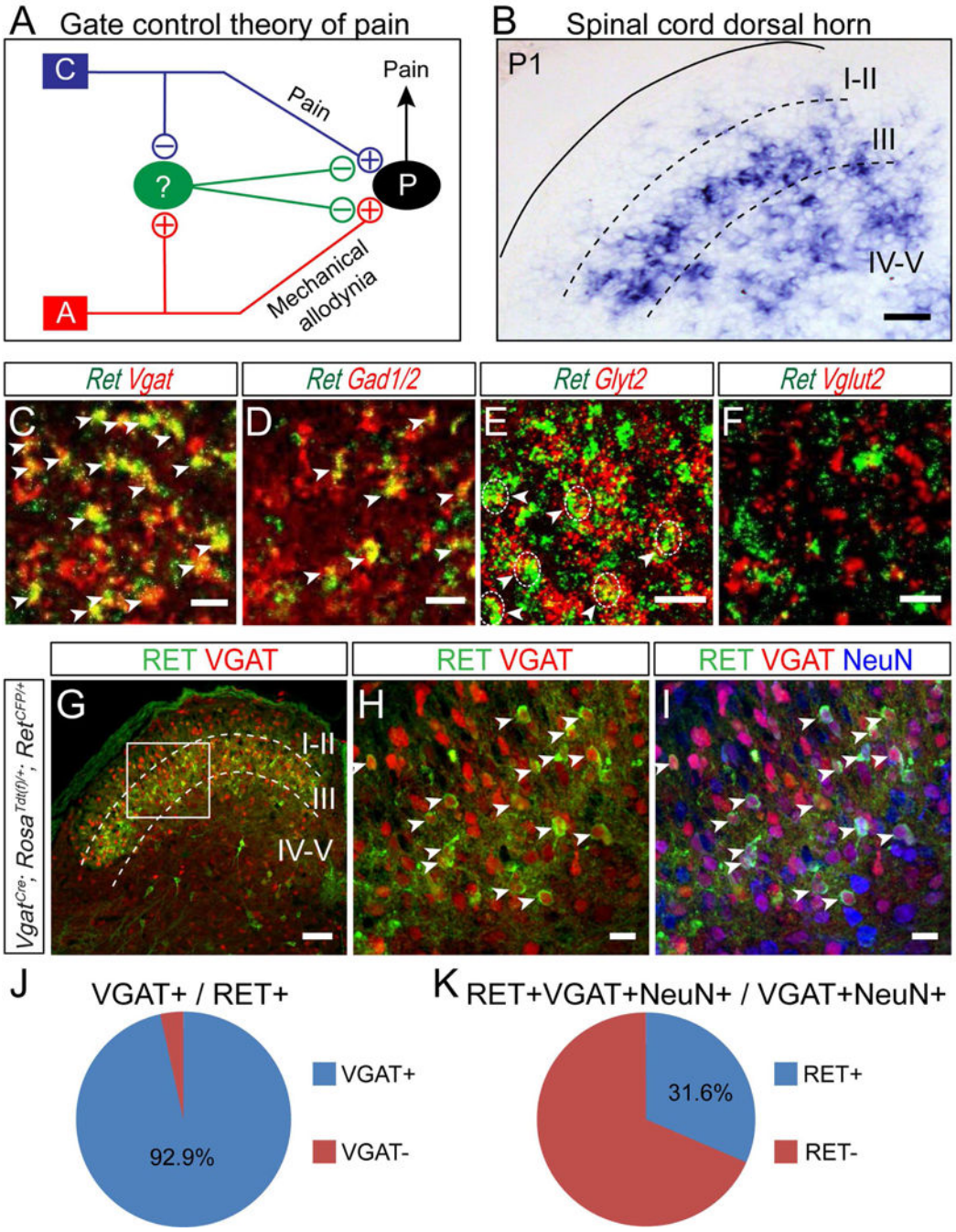

Figure 1. Molecular characterization of early RET+ dDH neurons

(A) Schematic showing the "gate control theory" of pain. "C" represents the nociceptive C fiber; "A" represents the mechanosensitive Aβ fiber; "P" represents the projection neuron; the green oval represents the "gating" neuron; and "+" and "−" indicate excitatory and inhibitory connections. (B) *In situ* hybridization of *Ret* in a P1 transverse section of lumbar spinal cord. Scale bar, 50 μm. (C–F) Double fluorescent *in situ* hybridization of *Ret* and inhibitory neuronal markers *Vgat*, *Gad1/2*, *Glyt2*, or the excitatory neuronal marker *Vglut2*. Arrowheads indicate examples of double positive cells. Dashed circle outlined some *Ret/*

Glyt2 double positive cell bodies. Scale bars, 20 μm. (G–I) Triple staining of Tdt (red) and antibodies against GFP (green) and NeuN (blue) with P7 lumbar spinal cord section of $Vgat^{Cre}$; $Rosa^{Tdt(f)/+}$;$Ret^{CFP/+}$mice. Arrowheads indicate some double or triple positive cells. Scale bars, 100 μm (G) and 20 μm (H and I). (J and K) Quantification of triple staining. 6–8 sections/mouse, n=3 mice.

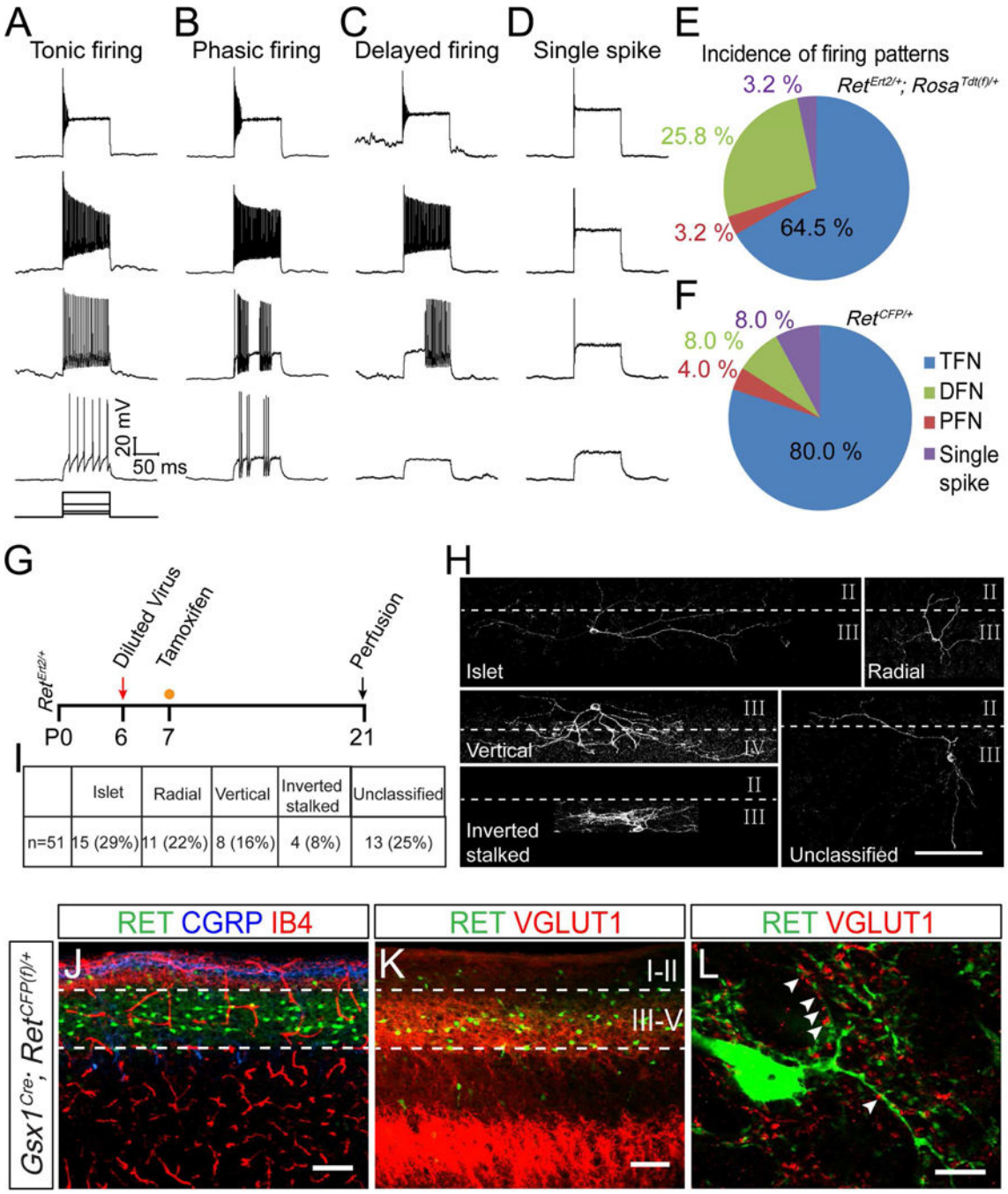

Figure 2. Physiological, morphological, and anatomical characterization of early RET+ dDH neurons

(A–D) Firing patterns of genetically traced early RET+ dDH neurons in *Ret*$^{Ert2/+}$; *Rosa*$^{Tdt(f)/+}$ mice or RET+ dDH neurons in *Ret*$^{CFP/+}$ mice, which are revealed by rectangular current injection of 30, 60, 150, and 300 pA. Vh=−70 mV. (E and F) Pie graphs showing the proportion of each firing pattern. 31 and 25 cells were recorded from four mice of each genotype. (G) Schematic showing the timeline of intraspinal AAV-Flex-ChR2-EYFP virus injection and tamoxifen treatment for sparse labeling of early RET+ neurons. (H) Representative morphologies of genetically traced early RET+ dDH neurons at P21. Dashed

lines indicate the border between lamina. Scale bar, 100 μm. (I) Summary of the incidence of each defined morphology. (J–L) Sagittal spinal cord sections of P7 *Gsx1*^{Cre}; *Ret*$^{CFP(f)/+}$ mice. (J) Most RET+ neurons are located ventral to peptidergic (CGRP+) and non-peptidergic (IB4+) primary afferent innervation. (K) RET+ DH neurons are surrounded by VGLUT1+ puncta. (L) Enlarged image shows that RET+ neurons make contact with VGLUT1+ puncta (arrowheads). Scale bars, 100 μm (J and K) and 10 μm (L).

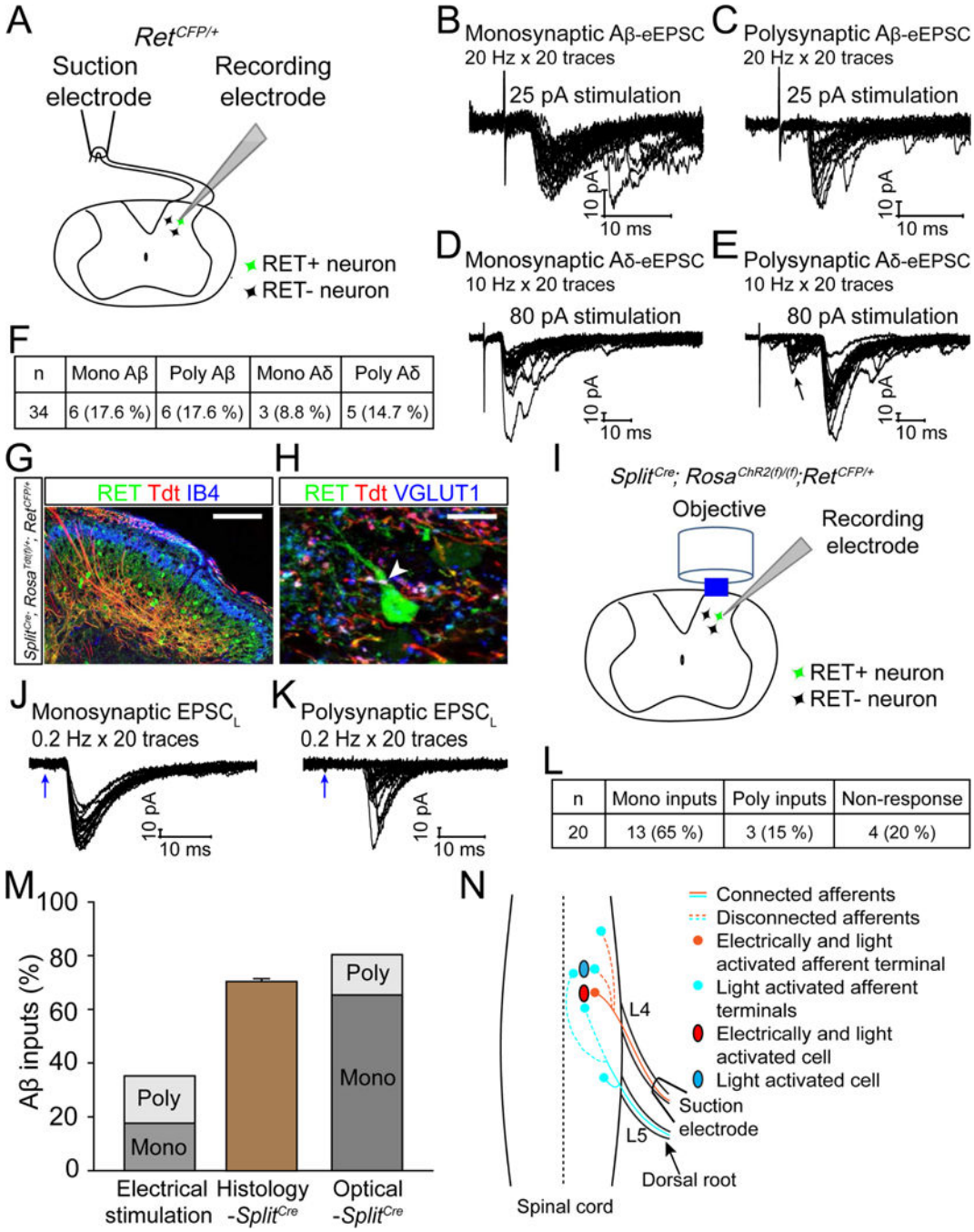

Figure 3. RET+ dDH neurons receive Aβ mechanosensory inputs

(A) Schematic of evoked EPSC recording. (B–E) Representative traces of Aβ- and Aδ-evoked EPSCs of RET+ dDH neurons induced by high frequency stimuli. We defined monosynaptic Aβ- or Aδ-eEPSCs as stable latency and an absence of synaptic failure during 20 Hz or 10 Hz stimuli, respectively. Otherwise, the response was categorized as polysynaptic. Left: monosynaptic inputs; right: polysynaptic inputs (arrow in E indicates when polysynaptic Aδ responses occur). (F) Quantification of mono- and polysynaptic A inputs onto recorded RET+ dDH neurons by electrical stimulation. (G and H) Triple staining

of spinal cord sections of 3pw *Split*^{cre}; *Rosa*$^{Tdt(f)/+}$; *Ret*$^{CFP/+}$ mice with IB4 (G) or VGLUT1 (H). A Tdt+/VGLUT1+ punctum is indicated by a white arrowhead. Scale bars, 100 μm (G) and 10 μm (H), n=3 mice. (I) Schematic of light-induced EPSC recording from RET+ dDH neurons using spinal cord sections of 4pw *Split*^{Cre}; *Rosa*$^{ChR2(f)/(f)}$; *Ret*$^{CFP/+}$ mice. (J–K) Representative traces of 0.2 Hz light-induced EPSCs ($EPSC_{LS}$). Mono or polysynaptic $EPSC_{LS}$ were differentiated by 0.2 Hz, 20 times light stimulation. We classified a connection as monosynaptic if the $EPSC_{LS}$ latency jitter was < 1.6 ms. The blue arrows indicate laser stimuli. (L) Quantification of mono- and polysynaptic Aβ inputs onto recorded RET+ dDH neurons upon light stimulation. (M) Comparison of the percentage of RET+ dDH neurons showing Aβ inputs using electrical, histological, and optical approaches. (N) Schematic showing DH innervation of Aβ afferents.

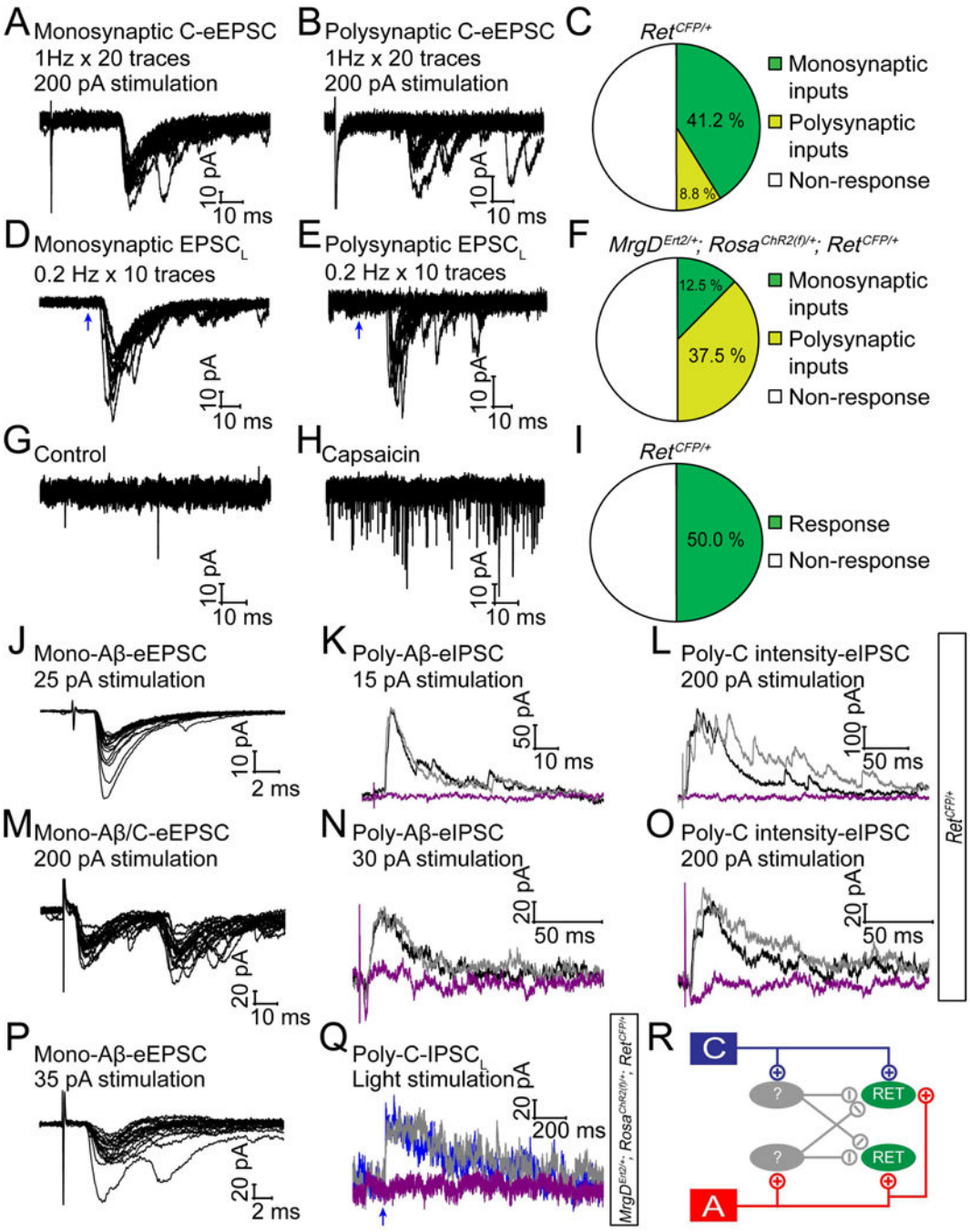

Figure 4. RET+ dDH neurons receive C fiber nociceptive inputs

(A and B) Representative traces of mono- and polysynaptic EPSCs of RET+ dDH neurons, evoked by 1 Hz C fiber stimulation of the dorsal root. A lack of synaptic failures during 1 Hz stimulation indicated a monosynaptic response, otherwise it was considered as a polysynaptic response. (C) Quantification of C fiber induced responses. (D and E) Light-induced EPSC recording from RET+ dDH neurons in 3–5pw *MrgD*$^{Ert2/+}$; *Rosa*$^{ChR2(f)/+}$; *Ret*$^{CFP/+}$mice. Mono or polysynaptic $EPSC_{LS}$ were differentiated by 0.2 Hz, 20 times light stimulation. (F) Quantification of light-induced responses. (G and H) 1 μM capsaicin

induced responses of RET+ dDH neurons in 4–5pw $Ret^{CFP/+}$ transverse/sagittal spinal cord slices. (I) Quantification of capsaicin induced responses. (J–O) Two examples of RET+ dDH neurons from 3–5pw $Ret^{CFP/+}$mice, which received monosynaptic excitatory Aβ inputs (J, holding potential −70 mV), or monosynaptic excitatory Aβ and C inputs (M), as well as polysynaptic inhibitory inputs by dorsal root stimulation of Aβ intensity (K and N, holding potential 0 mV) or C intensity (L and O). These inhibitory inputs (black traces) were blocked by strychnine (purple trace), but not by bicuculline (gray trace). (P–Q) An example of a RET+ dDH neuron in a 3–5pw $MrgD^{Ert2/+}$; $Rosa^{ChR2(f)/+}$; $Ret^{CFP/+}$ mouse, which received monosynaptic Aβ excitatory inputs upon dorsal root stimulation (P) as well as polysynaptic C inhibitory inputs by light stimulation (Q). The inhibitory inputs were blocked by strychnine (purple trace) but not bicuculline (gray trace) (Q). (R) Schematic showing inputs to RET+ dDH neurons.

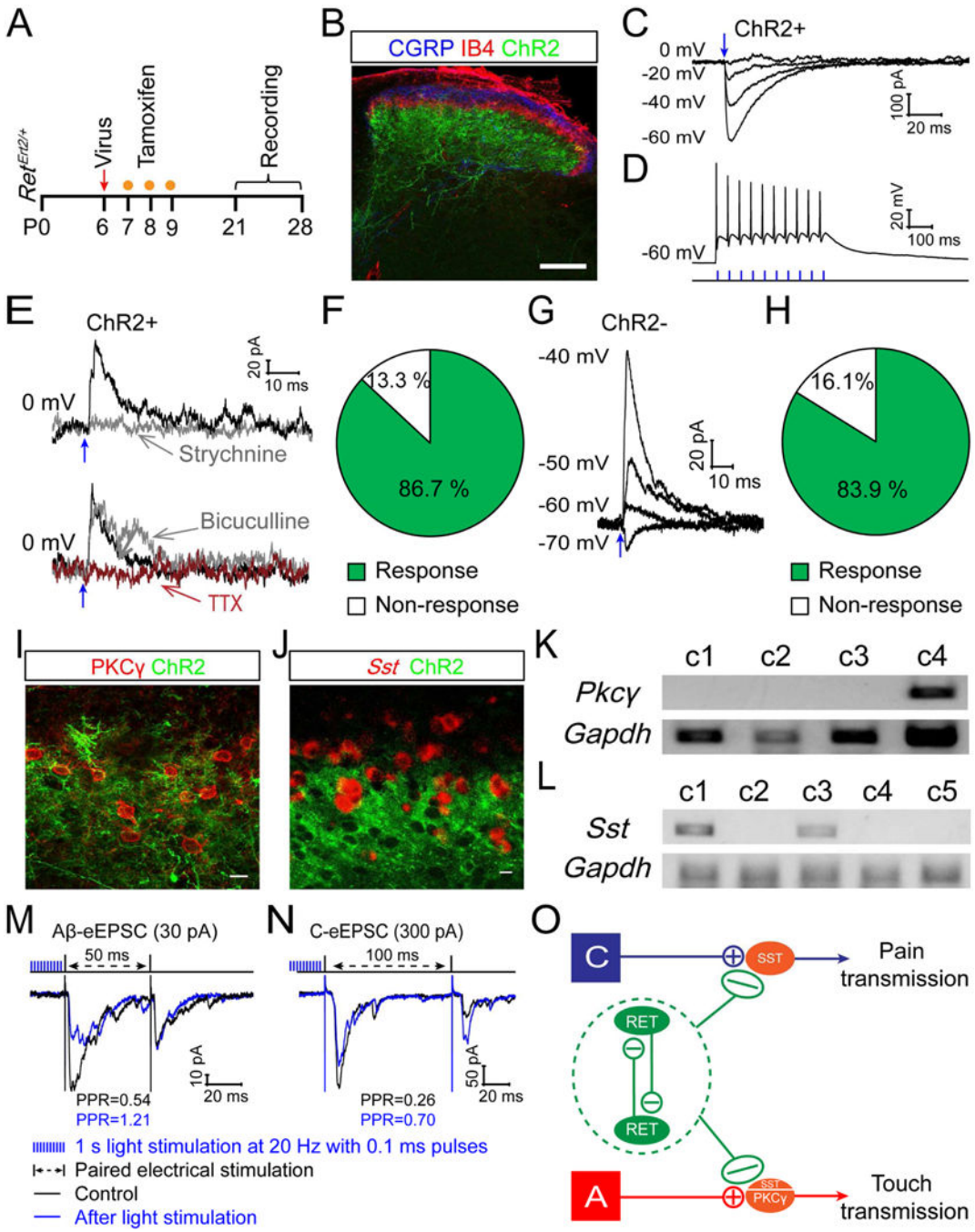

Figure 5. Outputs of early RET+ dDH neurons

(A) Schematic showing the timeline of intraspinal AAV injection, tamoxifen treatment, and recording. (B) Triple staining of EYFP, anti-CGRP, and IB4 with the transverse lumbar spinal cord section of a P21 *Ret*$^{Ert2/+}$*;AAV1-Flex-ChR2* mouse. Scale bar, 100 μm. (C) Representative traces of photocurrents of a ChR2+ neuron at different holding potentials. The reversal potential is around 0 mV. (D) A representative trace of action potentials from a ChR2+ neuron upon 20 Hz light stimulation in current clamp mode. (E and F) 86.7% (13/15) of the recorded ChR2+ neurons showed light-induced IPSCs ($IPSC_{LS}$) at 0 mV

holding potential, which were blocked by strychnine (0.4 μM) or TTX (1 μM) but not by bicuculline (10 μM). (G and H) 83.9 % (26/31) of the recorded ChR2 negative neurons, which are adjacent to the ChR2+ neurons, showed $IPSC_{LS}$. These $IPSC_{LS}$ possessed reversal potentials between −60 to −70 mV. (I) Double staining of EYFP and PKCγ shows that ChR2+ neurites surround PKCγ+ cell bodies. (J) A combination of fluorescent *in situ* hybridization of *Sst* and immunostaining of EYFP shows that ChR2+ neurites surround SST + cell bodies. Scale bars, 10 μm. (K–L) Representative single cell RT-PCR results for *Pkcγ* and *Sst* from responsive ChR2 negative neurons. (M–N) Paired pulse recordings from ChR2 negative layer I–II neurons of $Ret^{Ert2/+}$;*AAV8-Flex-ChR2* spinal cord slices. DH neurons were chosen if they received monosynaptic Aβ (M, 30 pA) or C (N, 300 pA) inputs but do not display light-induced postsynaptic responses. Note that before light stimulation, paired-pulse stimuli induced a depression of the second EPSC. However, optical stimulation (1 second light at 20 Hz with 0.1 ms pulses) inhibits the first response but increases the second one. (O) Schematic showing outputs of early RET+ dDH neurons: 1) inhibiting other RET+ dDH neurons; 2) inhibiting SST+ or PKCγ+ excitatory interneurons postsynaptically; and 3) inhibiting primary afferents presynaptically.

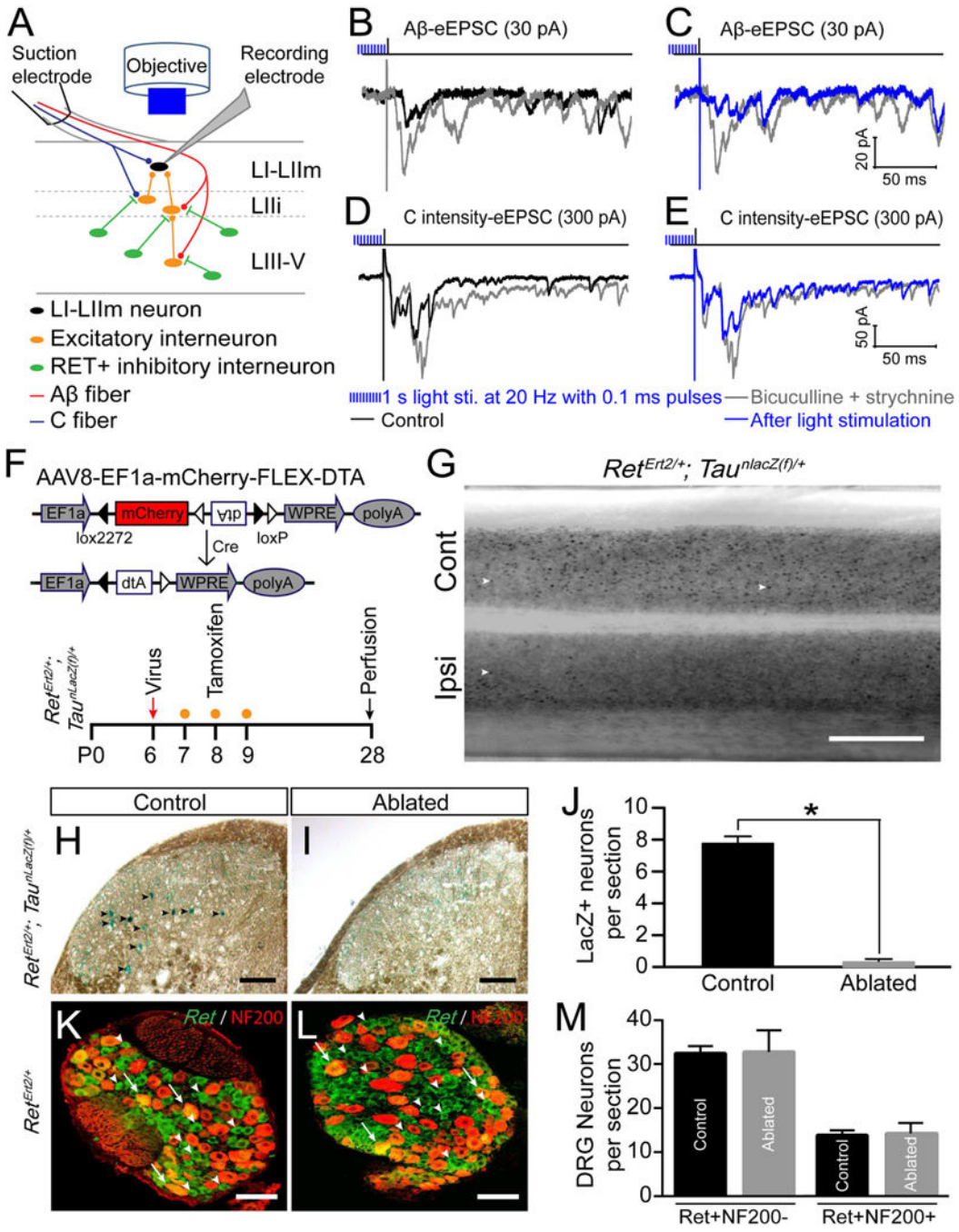

Figure 6. Activation of early RET+ dDH neurons blocks hyperactivity of A and C pathways and specific ablation of early RET+ dDH neurons

(A) Schematic showing polysynaptic EPSC recording from DH layer I–II neurons of 3–4pw *RetErt2/+; AAV8-Flex-ChR2* mice upon pharmacological dis-inhibition. Primary afferents were activated by electrical dorsal root stimulation using Aβ or C intensities, while light stimulation (1 second light at 20 Hz with 0.1 ms pulses) was applied to activate early RET+ dDH neurons. (B) Representative traces of Aβ-eEPSCs recorded from a layer IIi neuron by 25pA dorsal root stimulation. Upon 10 μM biuculline and/or 0.4 μM strychnine perfusion, Aβ-eEPSCs dramatically increased, especially the polysynaptic components. (C) This

increase of Aβ-eEPSCs upon dis-inhibition was significantly blocked by light stimulation. (D) Representative traces of a layer IIm neuron upon 300 pA dorsal root stimulation. This neuron received both monosynaptic Aβ and C inputs in normal condition. Upon pharmacologic dis-inhibition, C intensity triggered polysynaptic components increased. (E) This increase of C intensity triggered eEPSCs was greatly blocked by light stimulation. (F) Schematic showing DNA structure of AAV8-Flex-DTA and the timeline of intraspinal virus injection, tamoxifen treatment, and analysis. (G) Dorsal view of whole mount lumbar spinal cord LacZ staining from an AAV8-Flex-DTA injected 4pw $Ret^{Ert2/+}$; Tau^{nLacZ} mouse. Examples of LacZ+ neurons are indicated by white arrowheads. Cont, Contralateral side; Ipsi, ipsilateral side. Scale bar, 0.5 mm. (H–I) LacZ staining of ipsilateral lumbar dorsal spinal cord sections of control 2 and DTA Abl mice. LacZ+ neurons are indicated by black arrowheads. Scale bars, 100 μm. (J) Quantification of LacZ+ neurons in control (7.8 ± 0.5/section) and DTA Abl (0.3 ± 0.1/section) mice. 8–10 horizontal sections per mouse were counted around the L4 injection site. N=4 mice per group, $p < 0.05$, student's unpaired t test. Data are represented as mean ± SEM. (K–L) Representative images of fluorescent *in situ* hybridization of *Ret* and immunostaining of NF200 with ipsilateral L4/L5 DRG sections of control (K) and DTA Abl mice (L). Scale bars, 50 μm. (M) Quantification of RET+/NF200+ and RET+/NF200− L4 DRG neurons in control and DTA Abl mice. $p > 0.05$, student's unpaired t test. 4–5 sections/mouse and n=3 mice/group.

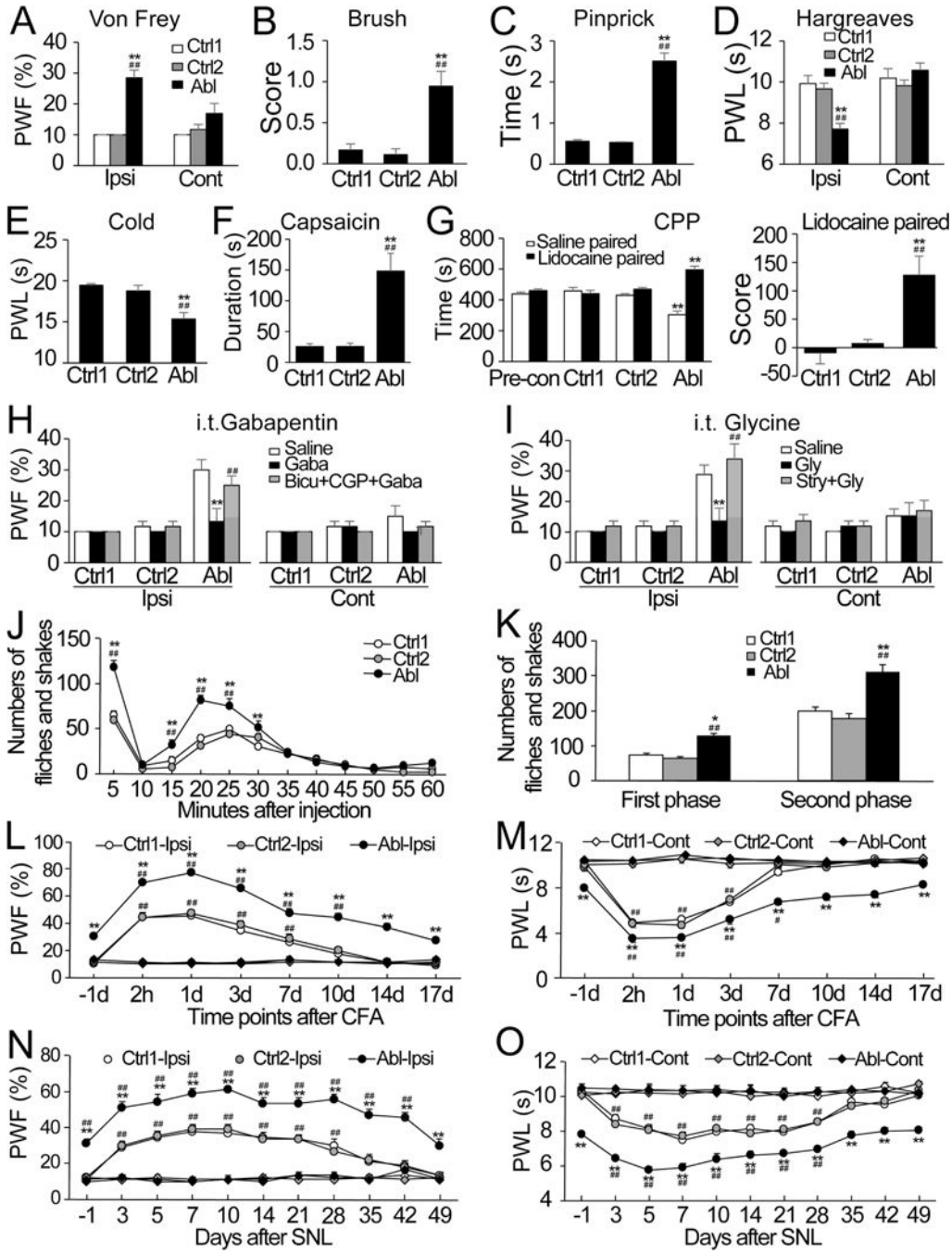

Figure 7. Specific ablation of early RET+ dDH neurons increases basal pain perception and augments inflammatory and neuropathic pain in adult male mice

(A) A significant increase in paw withdrawal frequency (PWF) to static mechanical stimulation (0.07 g) was observed on the ipsilateral (Ipsi), but not contralateral (Cont), side of DTA ablated (Abl) mice (n=13) as compared to control group 1 (Ctrl1; n=9) or control group 2 (Ctrl2; n=6). $^{**}p < 0.01$ *vs* the corresponding Ctrl1 and $^{\#\#}p < 0.01$ *vs* the corresponding Ctrl2. (B and C) Marked increases in dynamic allodynia score to a smooth paint brush (B) and in paw withdrawal duration to noxious mechanical stimulation by a safety pin (C) were observed on the ipsilateral side of DTA Abl mice (n=6 in B; n=12 in C)

as compared to Ctrl1 (n=6 in B; n=9 in C) or Ctrl2(n=6 in B; n=6 in C). $^{**}p < 0.01$ *vs* the corresponding Ctrl1 and $^{\#\#}p < 0.01$ *vs* the corresponding Ctrl2. (D and E) Profound reductions in paw withdrawal latency (PWL) to noxious heat (D) and cold (0°C; E) were observed on the ipsilateral but not contralateral side of DTA Abl (n=9/treatment) as compared to Ctrl1 (n=6/treatment) or Ctrl2 (n=6/treatment) mice. $^{**}p < 0.01$ *vs* the corresponding Ctrl1 and $^{\#\#}p < 0.01$ *vs* the corresponding Ctrl2. (F) A significant increase in the duration of paw licking/lifting within 5 min was observed after capsaicin injection on the injected side of DTA Abl as compared to Ctrl1 or Ctrl2mice. n=5/group. $^{**}p < 0.01$ *vs* the corresponding Ctrl1 and $^{\#\#}p < 0.01$ *vs* the corresponding Ctrl2. (G) Left panel: The DTA Abl mice (n=7) displayed an increase in the time spent in the lidocaine paired chamber and a corresponding decrease in the saline paired chamber. The Ctrl1 (n=6) or Ctrl2 (n=6) mice showed no chamber preference. $^{**}p < 0.01$ *vs* the corresponding pre-conditioning (Pro-con) values. Right panel: Difference scores confirmed that DTA Abl mice, but not Ctrl1 and Ctrl2 mice, displayed the preference for the lidocaine chamber. $^{**}p < 0.01$ *vs* the corresponding Ctrl1 and $^{\#\#}p < 0.01$ *vs* the corresponding Ctrl2. (H and I) A significant increase in PWF on the ipsilateral side of DTA Abl mice was abolished by intrathecal administration of gabapentin (Gaba, 50 μg/5 μl) or glycine (Gly, 100 μg/5 μl). These effects were completely reversed either by intrathecal co-administration of bicuculline (Bicu, 0.1 μg/5 μl) and CGP55845 (CGP, 0.1 μg/5 μl) or by intrathecal co-administration of strychnine (Stry, 1 μg/5 μl). n=6/treatment. $^{**}p < 0.01$ *vs* the corresponding saline-treated DTA Abl mice and $^{\#\#}p < 0.01$ *vs* the corresponding Gaba- or Gly-treated DTA Abl mice. (J and K) Numbers of formalin-induced licking and shaking in both the first and second phases of DTA ablated (Abl) mice were greater than those from Ctrl1 or Ctrl2 group. n=5/group. (J) Time course. (K) Summary of behaviors in the first and second phases. $^{*}p < 0.05$ or $^{**}p < 0.01$ *vs* the corresponding Ctrl1 and $^{\#\#}p < 0.01$ *vs* the corresponding Ctrl2. (L–O) The magnitudes and durations of CFA- (L and M) or SNL- (N and O) induced static mechanical allodynia (L and N) and thermal hyperalgesia (M and O) in DTA Abl mice were greater than those in either Ctrl1 or Ctrl2 mice. n=7/group in CFA and 9/group in SNL. $^{**}p < 0.01$ *vs* the corresponding time points in the Ctrl1 and $^{\#}p < 0.05$ or $^{\#\#}p < 0.01$ *vs* the corresponding baseline (−1d) on the ipsilateral side.

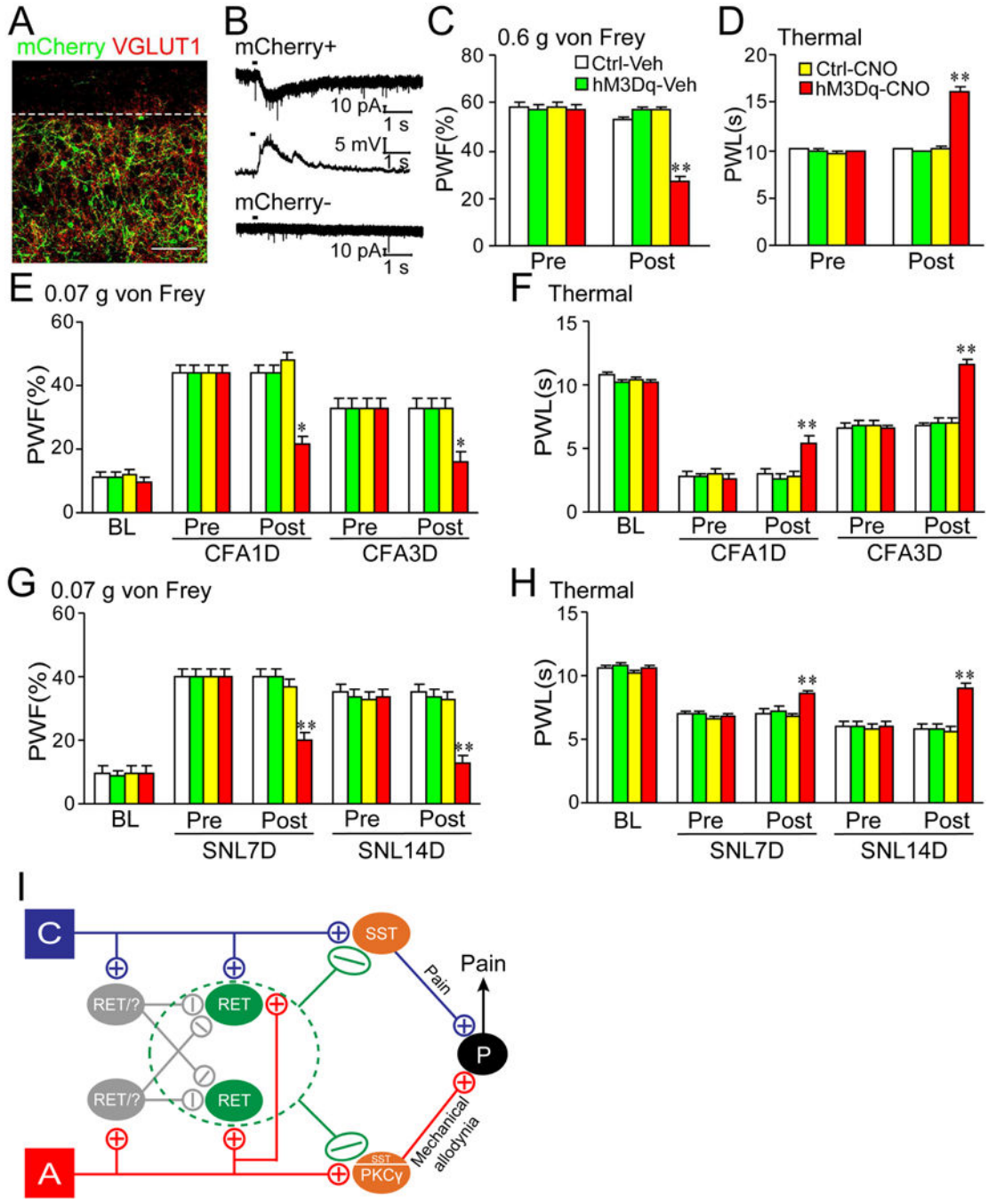

Figure 8. Acute activation of early RET+ dDH neurons reduces basal pain perception and attenuates inflammatory and neuropathic pain in adult male mice

(A) hM3Dq-mCherry is predominantly expressed in lumbar enlargement lamina III–V neurons of Ret^{Ert2} mice that were injected with AAV8-hSyn-DIO-hM3D(Gq)-mCherry. (B) mCherry+ (but not negative) neurons showed inward current in voltage clamp or membrane depolarization in current clamp upon CNO (3 mM) application. (C and D) A decrease in PWF and an increase in PWL were observed only in the hM3Dq mice post-CNO (5 mg/kg) injection. Ctrl: control 1 mice. Veh: vehicle (10% DMSO). n=12/group. $^{**}p < 0.01$ *vs* the corresponding pre-CNO injection (Pre). (E–H) CFA- (E and F) or SNL-(G and H) induced

increases in PWFs (E and G) and decreases in PWLs (F and H) were attenuated in the hM3Dq mice post-CNO injection at time points shown after CFA or SNL. BL: baseline. n=6/group. *$p < 0.05$ or **$p < 0.01$ *vs* the corresponding pre-CNO injection. (I) Schematic showing neuronal circuits related to early RET+ dDH neurons. They receive excitatory A and C primary afferent inputs as well as polysynaptic inhibitory inputs from A or C afferents through inhibitory interneurons (which may include RET+ dDH neurons themselves). They negatively modulate both pain and touch DH pathways by inhibiting primary afferents presynaptically and SST+ or PKCγ+ excitatory interneurons postsynaptically.